ORIGINAL SCIENTIFIC PAPER

CROATICA CHEMICA ACTA

Croat. Chem. Acta **2023**, *96*(2), 81–89
Published online: December 9, 2023
DOI: 10.5562/cca3961

HKD 1926

N,N-Dimethylamino Phenyl Curcumin Drug Loaded Polyethylene Glycol-Chitosan Incorporated Zinc Oxide Nanoparticles for Anti-Arthritic Activity

K. Priyadharsini,[1,2] M. Anbuchezhiyan[2,*]

[1] *Department of Physics, Tagore Engineering College, Rathinamangalam, Chengalpattu Dt., Tamil Nadu, India*
[2] *Department of Physics, SRM Valliammai Engineering College, Kattankulathur, Chengalpattu Tamil Nadu, India*
* Corresponding author's e-mail address: chezhiyan70@gmail.com

RECEIVED: January 31, 2023 * REVISED: September 3, 2023 * ACCEPTED: September 14, 2023

Abstract: Arthritis is a chronic autoimmune inflammatory disease in which healthy cells and tissues in the body are attacked by the body's own immune system. Inflammation leads to over- activation, differentiation and proliferation of lymphocytes. The aim of this study is to do *in-vitro* studies with Chitosan-Polyethylene glycol polymer-coated ZnO nanoparticles which carry NN-Dimethylaminocurcumin (NNDMA Cur) synthetic form of curcumin as the drug in the treatment of arthritis. The NNDMA Cur loaded Zinc Oxide nanoparticles were prepared using a hydrothermal method and characterized with certain techniques such as Powder X-ray diffraction, Fourier transform infrared, UV-Visible spectroscopy, Transmission electron microscope, Nuclear magnetic resonance, Electrospray ionization-Mass spectrum and *in-vitro* drug releasing studies. The obtained results proved that drug NNDMA Cur was continuously released, especially at pH 5.4, which is optimal for drug absorption by humans. The percentage of inhibition for the produced nanocomposite NNDMA Cur-PEG-CS-ZnO is determined to be effective for antiarthritic activity.

Keywords: chitosan, polyethylene glycol, NNDMA cur, NMR, ESI-mass spectrum, antiarthritic activity.

INTRODUCTION

In the recent days, the growth of human population poor life style ended with increasing toxic pollutants all around the nation and the accumulation of toxic contaminants inside human body.[1] These toxic contaminants alter the metabolism in human body and cause various kinds of complications. Pharmacotherapy has proven to be indispensable to overcome these problems. Many natural products are of plant origin and they play a vital role in human clinical trials. The intent of the current study is to synthesize, characterize and to treat arthritis with the synthetic analogue of curcumin and Dimethyl curcumin.[2] Curcumin is derived from the roots of Turmeric longa and it contains the active component of curcuminoids.[3] The utilization of traditional healing capabilities, using the nanotechnology's benefits: Curcumin is a good example of this.[4] Natural curcuminoids contain 77 percentage of curcumin, 17 percentage of demethoxy curcumin and 3 percentage of bisdemethoxy curcumin. Curcumin is a low molecular weight lyophilic compound with a wide range of collusive properties.[5] They have pleotropic activity and they are used in various industries such as food (as preservatives), fabric (as coloring agents) and in traditional medicine. The effect of curcumin depends on three active areas: a hepatonoid chain with a phenolic group, a double bond with cis-trans isomerism, a central keto group with a keto-enol tautomerism. Herbs synthesized from turmeric are widely used in pharmacology in both natural and artificial forms.[6]

Natural form of curcumin is called Yellow 3 and the synthetic form of curcumin is called Gelb 6. Natural curcumin is less soluble in water and highly soluble in acids and organic solvents, which is a barrier for therapeutic purposes.[7] Bioavailability of curcumin can be determined by its systemic distribution and its absorption capacity in the digestive tract. Curcumin's efficacy has been reduced due to its short plasma life span, low availability, decreased oral absorption, low solubility in gastric and other biological fluids, and instability at certain pH levels. To overcome the limitation a synthetic analogue Dimethyl curcumin

(DiMc1,7bis (3,4methoxyl phenyl)-1-6-heptaptadine,3-5dione) is used.

Dimethyl curcumin is a bioactive polyphenyl derivative[8] non-steroidal antiandrogen with high metabolic stability and it has properties such as antioxidant, antiasthmatic, antiapoptotic, anti-inflammatory, anticancer, antiproliferative, antifungal, antiviral and antibacterial properties.[9] Methylation of curcumin helps to improve its targeting skills and hydrophobicity. Synthetic curcumin is an effective means of eliminating free radicals such as nitrogen and oxygen and so they act as effective scavengers.[10] Synthetic curcumin and natural curcumin, although widely used, they have limitations due to poor oral availability, deterioration under normal physiological conditions and less solubility. Conditioning curcumin can increase solubility, which can be a promising alternative in therapeutics. Conventional bio enhancements are carried out to improve the properties of curcumin. Nano formulated curcumins are more effective than the native natural forms, because they have other properties such as high stability, long shelf life, lack of toxicity, high solubility, specific targeting ability and the controlled release of active ingredients. The conventional bio enhancements are carried out to improve the characteristics of curcumin.

Nano formulated curcumin helps to promote cell proliferation and it has a high anti- inflammatory effect.[11] It is used for cardiovascular disease, arthritis, skin, liver, bone, muscle and ailments. They inhibit mediators that trigger the inflammatory response, and block the proliferation of T lymphocytes.[12] This reduces matrix metal proteins and reduces the activation of macrophages and microglia.

The aim of this study is to do *in-vitro* studies with Chitosan-Polyethylene glycol polymer-coated ZnO nanoparticles which carry dimethyl curcumin as the drug in the treatment of arthritis.[13] Arthritis is a chronic autoimmune inflammatory disease in which healthy cells and tissues in the body are attacked by the body's own immune system. Inflammation leads to over- activation, differentiation and proliferation of lymphocytes.[14] Overactivation causes a storm of inflammatory cytokines and thus immune system imbalance and tissue damage.[15] This causes regional inflammation, which can harden the synovial membrane and destroy cartilage, bones and joints. Symptoms may vary from patient to patient depending on the severity. Inflammation can lead to the decreased apoptosis. Apoptosis is essential for maintaining body homeostasis.[16]

Chitosan, a mucopolysaccharide closely related to the polysaccharide cellulose is a natural polymer extracted from crustaceans and it has a greater potential for drug delivery.[17] Deacetylation of chitin (β1-4, N-acetyl-D-glucosamine) produces chitosan. It is a polycationic polymer which contains a mixture of $C_8H_{15}NO_6$ (amide derivative of monosaccharide glucose) and D glucosamine ($C_6H_{13}NO_5$).[18]

The amino group at C-2 position of glucosamine contributes to the functional and the structural properties[19] of chitosan and it is responsible for its biocompatibility, biodegradability, low immunogenicity, and antibacterial activity that make it an ideal delivery vehicle in delivering drug to the target site for drug delivery purpose.[20] The inclusion of nanoparticles supports transport of the polymer through the gastrointestinal tract and it aids in the controlled specific release of drugs at the target sites. It can also be due to the facts such as lack of toxicity, biocompatibility, ease of use and low cost.

These *n* amino group aid in wound healing and drug delivery. Chitosan has excellent properties[21] but it has less mechanical strength and flexibility.[22] To increase the mechanical strength and flexibility polyethylene glycol a synthetic polymer is crosslinked along with it and incorporated with ZnO nanocrystals.[23,24]

Polyethylene glycol is a hydrophilic, bio-comparable, non-immunogenic hydrophilic plasticizer and it is therefore ideal for blending with chitosan.[25] Polyethylene glycol tends to reduce particle aggregation and thus it helps to produce, store and apply nanoforms with high stability.[26] The addition of polyethylene glycol with metal nanoparticles (ZnO)[27] are biologically safe and biocompatible and they have different structural properties depending on their size, shape, morphology and orientation. PEG-modified ZnO nanoparticles are hydrophilic and induce apoptosis.[28,29]

EXPERIMENTAL

Preparation of Zinc Oxide (ZnO) Nanoparticles

Zinc (II) acetate (10 g) was treated with NaOH (0.83 g) in a 50 mL of ethylene glycol at under constant stirring for 30 min. The resulting white colored fluffy precipitate was transferred to a Teflon-lined autoclave at 180 °C for 12 h. The supernatant was discarded carefully and washed with distilled water by centrifuge technique for at least 10 times to completely remove the volatile impurities. The collected solid material was dried in water bath at 70 °C. The powder was annealed at 200 °C for 3 h and ground to get ZnO nanoparticles fine powder.

Preparation of Polyethylene Glycol-Chitosan polymer (PEG-CS)

The PEG-6000 (0.6 g) was mixed with tetrahydrofuran (30 mL) to that solution carbonyl diimidazole (0.6 g) is added and stirred for 30 min. To that mixture chitosan (0.2 g) is added and stirred for 3 h at 60 °C under nitrogen atmosphere. The mixture is cold to room temperature, filtered and dried in vacuum.

Preparation of Amine Coated Zinc Oxide (ZnO) Nanoparticles

ZnO nanoparticle powder weighing about 0.1 g was dissolved in 25 mL of double- distilled water, added to the APTES solution, and coated for 3 hours while being stirred. APTES (3-Aminopropyl triethoxysilane) coated nanoparticles were removed from solution by settling on the surface. It was washed thoroughly with water and dried for 3 h at 70–80 °C.

Preparation of PEG-CS Coated Zinc oxide NPs

The surface of ZnO nanoparticles was coated with a solution of PEG-CS to obtain the modified ZnO nanoparticles. In a typical experiment, 0.5 g of ZnO was dispersed in a surfactant containing CTAB (2 g of CTAB dissolved in 40 mL of deionized water) (Solution B). Then, 100 mL (0.02 g) CS-PEG with 1 % of acetic acid solution was slowly dropped into solution B. The mixture was continuously stirred with a rotational speed of 1000 rpm for 1 h at room temperature. Then, CS-PEG coated by ZnO nanoparticles was and thoroughly washed several times with ethanol and deionized water. Finally, the obtained CS-PEG coated ZnO nanoparticles were dried overnight at 60 °C.

Preparation of *N,N*-Dimethyl Curcumin (NNDMA)-PEG-CS-ZnO Nanoparticles

The *N,N*-dimethyl curcumin is synthesized by reported method.[30] 100 mg CS-PEG coated ZnO nanoparticles is dispersed in distilled water and sonicated for 15 min. 1 mg of *N,N*-dimethyl curcumin is dissolved in ethanol and then added drop wise to the PEG-CS-ZnO nanoparticle suspension and stirring continued for 12 h. NNDMA-loaded solution is subsequently collected by centrifugation at 4000 rpm. As before, a warm water bath was used to evaporate the solvent and concentrate the nano precipitate. Finally, the NNDMA-PEG-CS-ZnO is obtained as a fine powder.

Kinetic Studies of *in-vitro* NNDMA Cur Release

At 37 °C, three different phosphate buffers (pH: 5.4, 6.0, and 7.4) with a molarity of 0.2 M were used to study the kinetic investigations of NNDMACur release from PEG-PMMA- ZnO with respect to time. With a 12000 Da 020 molecular cut off, a dialysis membrane tube was filled with 10 mg mL^{-1} of the produced nanomaterials (Himedia, Dialysis membrane-110). At a setting of 37 °C, a beaker filled with 50 mL of PBS buffer was used to dip the dialysis tube in to 2 mL of the solution was taken out of the release medium at different times and replaced with brand-new phosphate buffer solution. A UV-Vis spectrophotometer (Diode-Array spectrophotometer 8453) was utilized to determine the absorbance of the release medium at various time intervals to determine the amount of curcumin released.

In Vitro drug Loading and Encapsulation Efficiency

To investigate the maximal encapsulation and the drug loading effectiveness of NNDMA Cur-PEG-CS-ZnO, the quantity of ZnO and the synthetic curcumin concentration were optimized. Following the completion of the experiment, the leftover solution containing synthetic curcumin was extracted using 5 mL of ethanol and water mixture (1 : 4), and its absorbance was determined using UV-Visible spectroscopy. During its loading, different volumes of synthetic curcumin solution were collected at equal intervals for measurement. Equations [Eq. (1)] and [Eq. (2)] were used to compute drug loading and encapsulation efficiency respectively

$$DLP = \frac{m_d}{m_{NP}} \times 100 \quad (1)$$

$$DLE = \frac{m_d}{m_{d,syn}} \times 100 \quad (2)$$

where m_d is the mass of drug loaded into the carrier, m_{NP} is the total mass of the drug-loaded nanoparticles, and $m_{d,syn}$ is the amount of drug utilized in synthesis and LP and LE are loading percentage and loading efficiency. The UV-Vis Agilent 8453 diode-array spectrophotometer was used to measure curcumin, which was identified at 430 nm. To measure the quantity of synthetic drug NNDMA Cur present in the ZnO, 1 mg of synthesized nanomaterials were dispersed in the water and ethanol mixture in the ratio of 1 : 1. The analyses were carried out in the UV-Visible spectroscopy at the wavelength of 430 nm.

Protein Denaturation Assay

The anti-arthritic activity of NNDMA Cur-PEG-CS-ZnO and conventional diclofenac sodium were tested utilizing the suppression of albumin denaturation procedure with minimal modifications. The conventional drug (NNDMACur) and PEG-CS-ZnO were dissolved in a small amount of dimethyl formamide (DMF) and diluted with phosphate buffer (0.2 M, PH 6.3). DMF was present in less than 2.5 percent of the whole solution. Test Solution (4 mL) containing various drug doses was combined with 1 mL of 1 mM Bovine serum albumin solution in phosphate buffer and it was incubated for 15 min at 37 °C in an incubator. The reaction mixture was kept at 70 °C in a water bath for 30 min to produce denaturation. The turbidity was measured at 660 nm after cooling. The percentage of denaturation inhibition was estimated from the control group in which no drug was used. The following formula was used to compute the percentage inhibition of denaturation:

$$\text{Percentage of Inhibition} = 100\frac{A_c - A_t}{A_c}$$

where A_c is absorbance of control and A_t is absorbance of test.

Physical Characterization

Powder X-ray diffraction was used with a Bruker X-ray diffractometer (AXS D8 Advance), USA, utilizing a Cu tube (= 1.5406), and Xpert High Score plus software to analyze the structure and the morphology of the resultant particles. The Agilent 8453 diode-array spectrophotometer, manufactured in the USA, was used to obtain the UV-Vis absorption spectra. A TF 20: Tecnai G2 200kV TEM (FEI), USA, was used for the TEM. A drop of the sample, suspended in ethanol, was applied to a copper grid that had been coated with carbon to create an electron-transparent specimen. Shimadzu's instrument 8400S was used to examine FT-IR spectra between 4500 and 350 cm^{-1}. Hydrogen 1H NMR (300 MHz CDCl3) and carbon NMR 13C NMR (75 MHz) NMR spectra for NNDMA Cur were performed in a 300 MHz high resolution NMR equipment.

RESULTS AND DISCUSSIONS

In this work, the synthesized biocompatible (NNDMA Cur) PEG-CS/ZnO nanoparticles for the effective drug delivery applications. Here, ZnO nanoparticles were used as the nanocarrier loaded with co-polymer PEG-CS for the stable drug releasing inside the target site. NNDMA Cur loaded on the nanocarrier via hydrophobic interactions. Under the acidic conditions the carboxylic acid present in the co-polymer (PEG-CS) weakens the bond between the polymers and ZnO, consequently the organic drug starts releasing from the nanocomposite (NNDMA Cur /PEG-CS/ZnO bionanocomposite). In the drug releasing studies (*in-vitro*) the results are observed when the NNDMA Cur-PEG-CS/ZnO nanoparticles are associated with other physical values like pH 7.2 and 6, the extraordinary drug releasing was observed at the rate of pH 5.4 (acid range) which is shown in scheme 1. This condition is well applicable for the sustained and the controlled release of NNDMA Cur to the targeting sites.

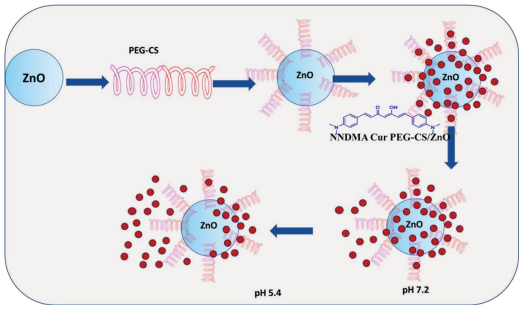

Scheme 1. Overall scheme of synthesis of NNDMA Cur-CS-PEG-ZnO and the mechanism of releasing of NNDMA Cur at the Inflammatory site.

Structural Analysis

The crystallinity of the samples was examined by X-ray diffraction and the peaks assignable to ZnO are observed in all the cases.[31] The lattice points are marked in Figure 1. The peak positions were shifted to higher 2Θ values for the polymer and the drug loaded ZnO as compared to bare ZnO. The particle sizes were linked to the broadness of the diffraction peaks. Particle sizes are calculated using Equation [Eq. (3)] known as Scherrer's equation as follows

$$d = k\frac{\lambda}{\beta}\cos\Theta \qquad (3)$$

where d is the crystalline size, k is Scherrer's constant (0.94), β is full width at half maximum of the peak (FWHM) and θ is diffraction angle. The average size of ZnO, ZnO/PEG-CS/ and for NNDMA Cur PEG-CS/ZnO synthesized nanoparticles was found to be 100, 113 & 115 nm respectively. The synthesized nanoparticles have a hexagonal wurtzite phase with the lattice constants $a = b = 0.3456$ Å and $c = 0.5389$ Å (JCPDS card no: 36−1451).[32] The d-spacing for NNDMA Cur PEG-CS/ZnO nanoparticles is found to be 0.2357 nm.

Spectral Analysis

UV-VISIBLE SPECTRAL ANALYSIS

Figure 2 illustrates, UV-Visible spectra of ZnO, polymer-coated ZnO, and synthetic drug (NNDMA Cur) loaded PEG-CS/ZnO bio-nanocomposite. The sharp absorption was

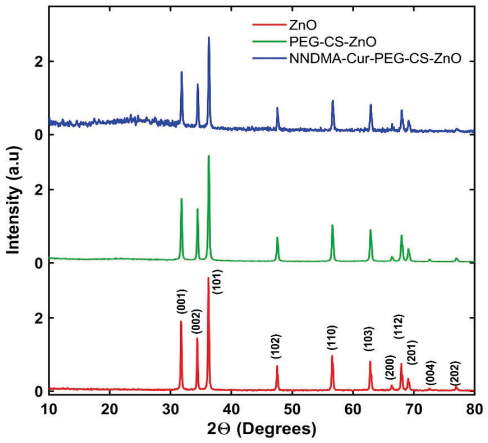

Figure 1. XRD pattern of synthesized nanoparticles.

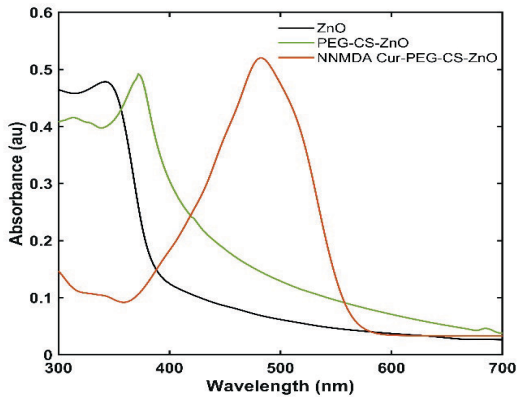

Figure 2. UV-Visible spectra of synthesized nanoparticles.

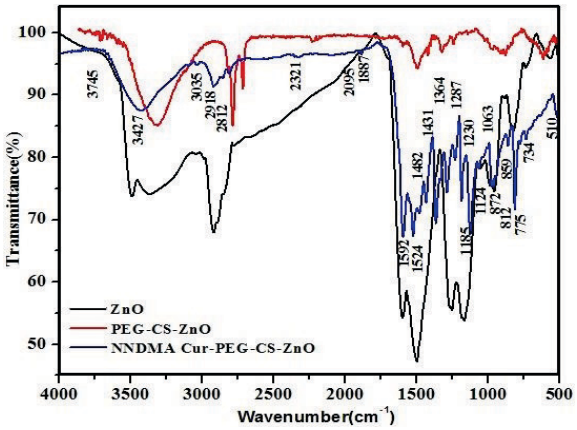

Figure 3. FTIR spectrum of synthesized nanoparticles.

observed at 342 nm for the as-prepared ZnO. The detailed theoretical analysis supported by experimental evidence reported earlier suggested that the obtained ZnO are tens of nanometers in size.[33,34] However, a red shift in the peak position with the narrowing of the absorption band is seen for PEG-CS polymer-coated ZnO. It is well known that the PEG is optically inactive in the spectral window of above 300 nm.[35] However, as revealed in the earlier reports, the chitosan moiety has been reported to absorb at about 310 nm.[36] The sharpness in the peak may be attributed to a better distribution of the nanoparticles under the influence of polymeric PEG-chitosan moiety. Further, the prominent absorption of curcumin is observed in the curcumin-loaded bio-nanocomposite. The observed peak at 480 nm is assignable to π→ π* transition of the drug molecule NNDMA. The shoulder at 340 in the absorption spectrum is due to the band edge absorption of ZnO nanoparticles.

FOURIER TRANSFORM - INFRARED SPECTRAL ANALYSIS

The FT-IR spectra of ZnO, Polymer coated ZnO & Drug loaded ZnO are shown in Figure-3. The IR spectrum of ZnO shows characteristic Zn-O bond vibration at 510 cm^{-1} attributed O-H stretching due to the presence of Zn-OH.[37] Further, the absorption band at 3510 cm^{-1} associated with a band at 2870 cm^{-1} is assignable to the presence of OH groups on the surface of ZnO. An additional broad band seen at 3400 cm^{-1} is due to the existence of defect site OH groups.[38] IR Absorption observed at 1096 cm^{-1} is due to C-O stretching and the band at 2812 is due to CH_2/CH asymmetric stretching of PEG.[39] Peaks at 1556 cm^{-1} and 1354 cm^{-1} belong to C=O stretching, N–H/C–N stretching of amide III and II of chitosan.[40] In the final composite, we observed all the above peaks in addition to the following absorptions attributed to NNDMA-Curcumin: 2918, 1513, 1422, 1102 cm^{-1}. The peak at 2918 cm^{-1} is due to enolic -OH group and the broad and weak absorption this peak indicates that the Curcumin involved hydrogen bonding with the polymer moiety. This is further evident from the shift of this peak position from the expected 2979 to 2918 cm^{-1}. The prominent band found at 1513 cm^{-1} is attributed to mixed vibrations of υ(C=O), δ(CC=O), and δ (CCC) of NNDMA-Curcumin. The band at 1422 cm^{-1} is assignable to deformation vibrations of methyl groups. The band of C-OH observed at 1230 cm^{-1} shows a shift towards lower wave-number from its expected position 1248 cm^{-1} due to inter-action of Curcumin with polymer functional units.

Morphological Analysis

The TEM images of NNDMA Cur PEG-CS/ZnO are shown in Figure 4, with different magnifications. After the effective inclusion of co-polymer with ZnO the loading of NNDMA Cur shows a little agglomeration among the particles and with the uneven shape. Prominently, the profile of the ZnO nanoparticles shows many substantial changes after loading with NNDMA Cur and co-polymer such as the clear presence of the co-polymer encapsulating layer on the ZnO nanoparticles. The average particle size was found to be 85 ± 13 nm. SAED pattern shows an amorphous nature due to the loading of co-polymers and NNDMA Cur.

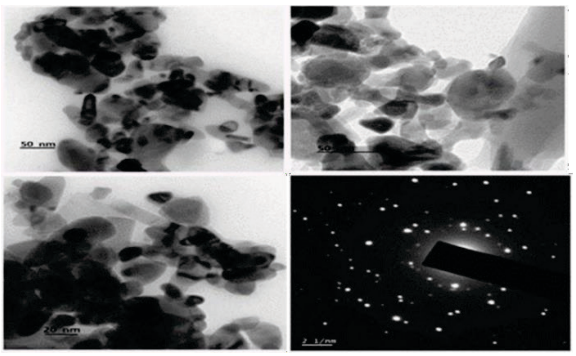

Figure 4. TEM image of NNDMA Cur PEG-CS/ZnO nanoparticles under different magnifications.

Nuclear Magnetic Resonance Spectroscopy (^{1}H NMR and ^{13}C NMR)

The signals for 25 protons are clearly visible in the ^{1}H NMR spectrum shown in Figure 5. The molecule has 26 protons. However, since the enolic proton is a labile proton, it does not appear in the spectrum. The presence of *N*,*N*-dimethyl units is indicated by the emergence of singlet for 12 protons around 3.0 ppm.

The enolic CH unit has a singlet at 5.72 ppm for one proton. For alkene protons that are close to the phenylene ring, a doublet at 6.4 ppm for two protons appears. For phenylene rings, doublets about 6.6 and 7.5 ppm for 8 protons (4 + 4 protons) occurred. Similarly, the presence of alkene protons close to the carbonyl unit is indicated by the development of a doublet at 7.6 ppm for two protons.

The NNDMA Cur includes nine sets of carbons, and the ^{13}C NMR clearly revealed the nine carbon signals which are shown in Figure 6. The presence of *N*,*N*-dimethyl carbon is shown by the carbon signal at 40.25 ppm. The existence of a carbonyl unit is shown by the signal at 183.43 ppm. The enolic carbon unit reached a peak of 101.00 ppm. The carbons of alkene and phenylene are found to remain as residual peaks.

NNDMA Cur has a molecular weight of 362 *m* / *z* and Figure 7 verifies that the positive mode signal is seen at 363 *m* / *z* in the ESI-Mass spectrum.

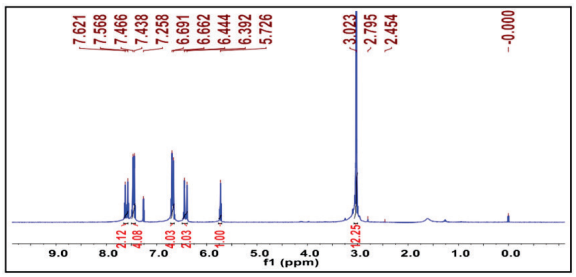

Figure 5. ^{1}H NMR spectrum of NNDMA Cur.

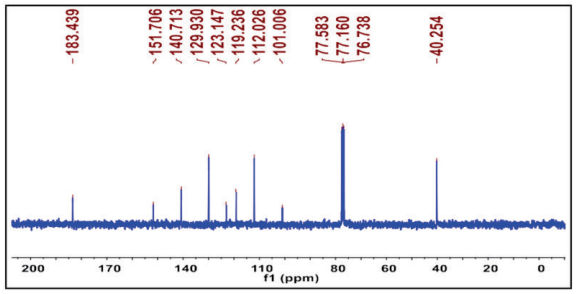

Figure 6. ^{13}C NMR spectrum of NNDMA Cur.

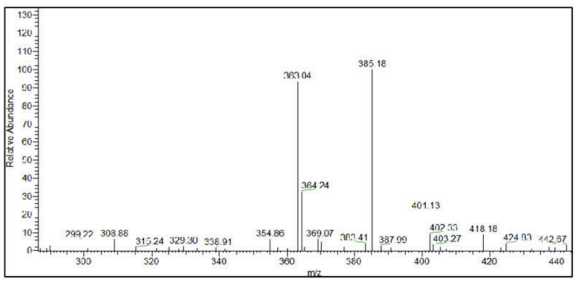

Figure 7. ESI-Mass spectrum of NNDMA Cur.

DFT Studies

To identify the interactions between PEG-CS and ZnO, PEG-CS-ZnO with *N*,*N*-dimethyl curcumin, the DFT studies is performed. The Gaussian 09W software is used to perform the

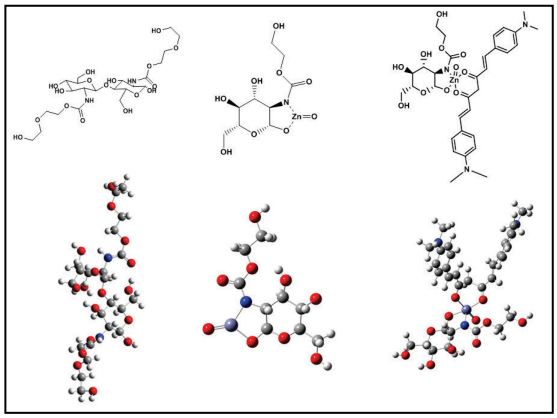

Figure 8. 2D and 3D structures of proposed interactions of PEG-CS, PEG-CS-ZnO and PEG-CS-ZnO *N*,*N*-dimethyl curcumin loaded composites.

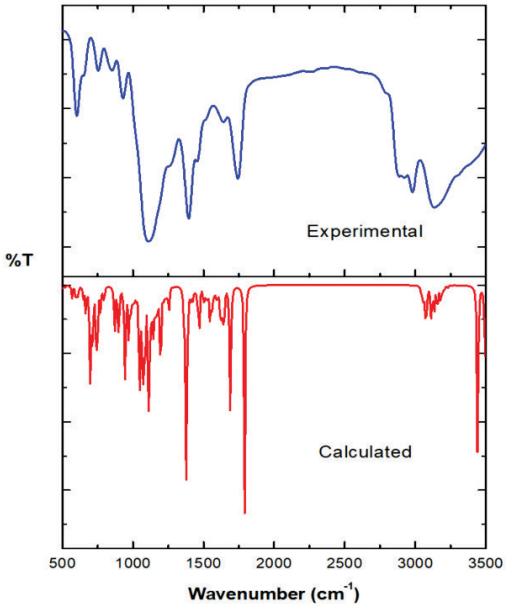

Figure 9. Experimental and calculated IR spectrum of PEG-CS.

optimization and frequency calculation with the basis set B3LYP/LAN2DZ or 6−31 g and Gauss view 5.0 software is used for visualize the results. The structures of PEG-CS, PEG-CS-ZnO and PEG-CS-ZnO composites are proposed and their frequencies are calculated and compared with experimental FT-IR spectrum. The calculated frequencies are exactly matching with experimental spectrum. Based on that result, the research is proposed that the ZnO forms interactions with the hydroxyl and NH units of PEG-CS. And also, the ZnO forms interactions with β-diketones carbonyls of the *N*,*N*-dimethyl curcumin. The interactions may form stable 5 membered and 6 membered ring. The proposed 2D and 3D structures of PEG-CS, PEG-CS-ZnO and PEG-CS-ZnO composite is given in Fig. 8. The observed and calculated spectrum and results are represented in Fig. 9−11 and Table. S1−S3 (Supporting Information).

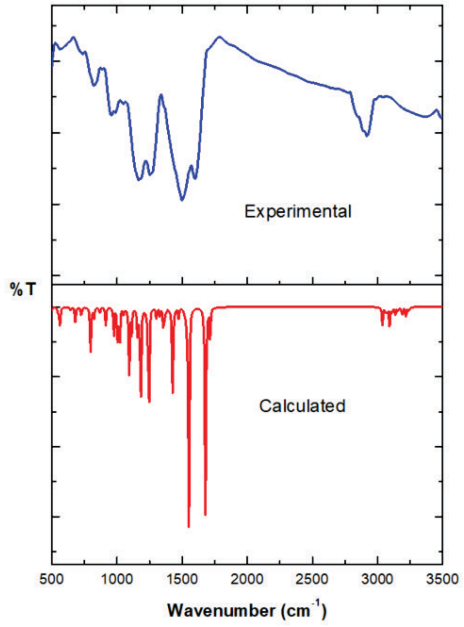

Figure 10. Experimental and calculated IR spectrum of PEG-CS-ZnO.

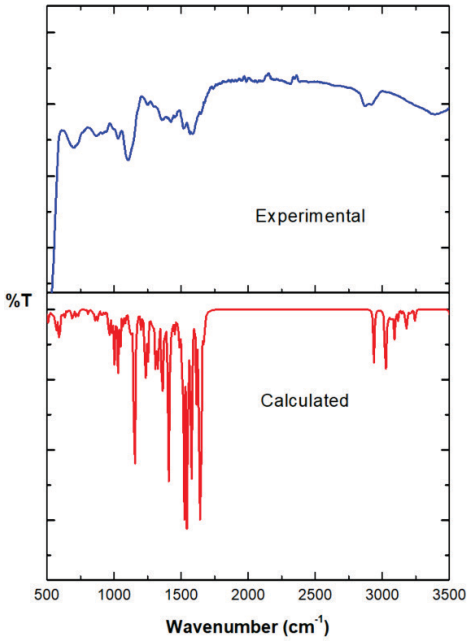

Figure 11. Experimental and calculated IR spectrum of PEG-CS-ZnO-*N*,*N*-dimethyl curcumin loaded composite.

Loading Efficiency (LE) and Loading Percentage (LP)

For calculating, the synthetic drug loading and the encapsulation efficiency of the synthesized nanoparticles were optimized using a UV-Vis spectrum. 500 µg of NNDMA Cur loaded on the PEG-CS/ZnO nanoparticles within 24 h and the calculated loading percentage and the encapsulation efficiency of synthetic curcumin using the [Eq. (1)] and [Eq. (2)] were found to be 23 % and 67 % respectively.

In-vitro Drug Release Studies

The *in vitro* drug release profile of NNDMA Cur and NNDMA Cur/PEG-CS/ZnO from the PEG-CS/ZnO nanoparticles in three different pH (5.4, 6 and 7.2) gradients at 37 °C is

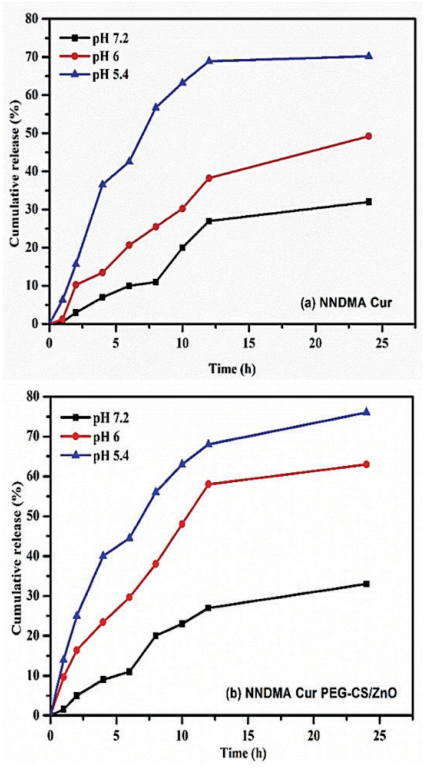

Figure 12. pH dependent release of synthesised nanoparticles of NNDMACur-PEG-CS/ZnO and NNDMA Cur.

depicted in Figure 12. It was efficiently released in the acidic environment, NNDMA Cur diffuse faster in acidic condition than the basic condition. Based on the drug release profile at pH 7.2, only 31 and 33 % of NNDMA Cur and NNDMA Cur/PEG-CS/ZnO were released and at pH 6, 63 %. Finally, pH 5.4 attained maximum drug release of 80 % at 24 hours clear from These data clearly show that the proportion of NNDMA Cur PEG-CS/ZnO nanoparticles released in the acidic buffer at pH 5.4 was extremely high.

Antiarthritic Activity

The anti-arthritic activity of the standard drug (diclofenac) and NNDMA Cur PEG- CS/ZnO are shown in Figure 9. Arthritis is caused by protein denaturation, which is a well-known cause. Autoantigens are produced when proteins are denaturated, causing significant inflammation in rheumatoid arthritis.[41] It is obvious from Table 1, in all concentrations, the synthesised nanoparticles are identical to the typical drug (diclofenac). Based on the findings, the prepared NNDMA Cur/PEG-CS/ZnO is capable of regulating the production of auto-antigens that cause protein denaturation during inflammation.

NNDMA Cur PEG-CS/ZnO nanoparticles are found to have an inhibitory concentration (IC50) of 100 g mL^{-1}, which is the same as the normal medication (diclofenac). The IC50 values of NNDMA Cur PEG-CS/ZnO and diclofenac sodium are found to be 96.33 µg mL^{-1} and 91.87 µg mL^{-1} respectively.

Table 1. Percentage of proteinase inhibitory activity of NNDMA Cur-PEG-CS-ZnO.

Concentration / µg mL^{-1}	% of proteinase Inhibitory Activity	
	NNDMA Cur-PEG-CS-ZnO	Diclofenac Sodium (Standard)
25	13.97 ± 1.04	16.21 ± 1.06
50	28.42 ± 2.02	30.37 ± 0.74
100	63.9 ± 1.20	65.09 ±0.86
150	76.27 ± 1.05	77.82 ±0.97
200	85.55 ± 1.06	87.91 ±0.74

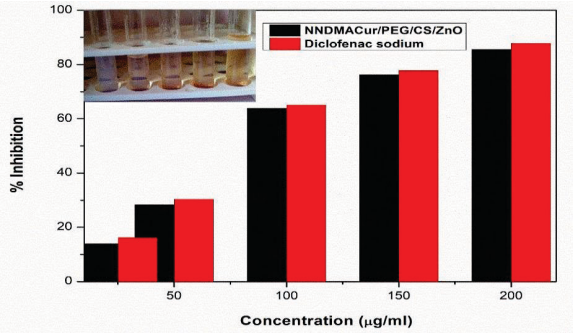

Figure 13. Anti-arthritic activity.

CONCLUSION

In this research work, NNDMA Cur-PEG-CS-ZnO has been successfully synthesized by a hydrothermal method. XRD study confirms the loading of synthetic curcumin with the decreased intensity without disturbing the crystalline nature. Interaction of NNDMA Cur with ZnO nanoparticles is confirmed by the shift at 480 nm which is obvious from UV-Visible analysis. Drug loading percentage (DLP) and drug loading efficiency (DLE) are found to be 23 % and 67 % respectively. The structures of PEG-CS, PEG-CS-ZnO and PEG-CS-ZnO composites are proposed and their frequencies are calculated and compared with experimental FT-IR spectrum. Based on that DFT studies result, the research is proposed that the ZnO forms interactions with the hydroxyl and NH units of PEG-CS. And also, the ZnO forms interactions with β-diketones carbonyls of the *N*,*N*-dimethyl curcumin which provides strong binding interaction between the NNDMA Cur and the nanocarrier. *In-vitro* drug releasing studies of NNDMA show the excellent loading, good efficiency and release of drug as compared to the individual NNDMA Cur. Therefore, the synthesized nanocomposite NNDMA Cur-PEG-CS-ZnO could be a probable material for arthritic therapy.

Supplementary Information. Supporting information to the paper is attached to the electronic version of the article at: https://doi.org/10.5562/cca3961.

PDF files with attached documents are best viewed with Adobe Acrobat Reader which is free and can be downloaded from Adobe's web site.

REFERENCES

[1] S. Yang, L. Liu, J. Han, Y. Tang, *Int.J. Cosmet. Sci.* **2020**, *42*, 16–28. https://doi.org/10.1111/ics.12592

[2] M. M. Yallapu, P. K. B. Nagesh, M. Jaggi, S. C. Chauhan, *AAPS Pharm. Sci.Tech. J.* **2015**, *17*, 1341–1356. https://doi.org/10.1208/s12248-015-9811-z

[3] T. Farooqui, A. Farooqui, *Curcumin: historical background, chemistry, pharmacological action, and potential therapeutic value*. In: Curcumin for Neurological and Psychiatric Disorders: Neurochemical and Pharmacological Properties (1st edition), Elsevier Inc, **2019**. https://doi.org/10.1016/B978-0-12-815461-8.00002-5

[4] A. Liakopoulou, E. Mourelatou, S. Hatziantoniou, *Toxicol. Rep*. **2021**, *8*, 1143–1155. https://doi.org/10.1016/j.toxrep.2021.05.012

[5] I. Chattopadhyay, K. Biswas, U. Bandyopadhyay et al, *Curr. Sci*. **2004**, *8*, 44–53.

[6] P. Anand, A. B. Kunnumakkara, R. A. Newman, B. B: Agarwal, *Mol. Pharm*. **2007**, *4*, 807–818. https://doi.org/10.1021/mp700113r

[7] D. Demirovic, S. I. S. Rattan, *Biogerontology*, **2011**, *12*, 437–444. https://doi.org/10.1007/s10522-011-9326-7

[8] R. S. Patwardhan, R. Checker, D. Sharma, et al. *Biochem. Pharmacol*. **2011**, *82*, 642–657. https://doi.org/10.1016/j.bcp.2011.06.024

[9] L. Zheng-yi, S. Dan-di, X. De-feng, et al., *Mod. Chem. Ind.* **2018**, *38*, 138–114.

[10] A. T. Iacob, F. G. Lupascu, et al. *Pharmaceutics* **2021**, *13*, 587. https://doi.org/10.3390/pharmaceutics13040587

[11] M. Gera, N. Sharma, et al. *Oncotarget* **2017**, *8*, 66680–66698. https://doi.org/10.18632/oncotarget.19164

[12] N. Ahmad, R. Ahmad, et al. *RSC Adv*. **2019**, *9,* 20192–20206. https://doi.org/10.1039/C9RA03102B

[13] R. Kugyelka, L. Prenek, et al. *Cells* **2019**, *8*, 504. https://doi.org/10.3390/cells8050504

[14] Y. Sun, W. Liu, et al. *J. Interferon Cytokine Res*. **2017**, *37*, 449–455. https://doi.org/10.1089/jir.2017.0069

[15] M. A. Moro-García, J. C. Mayo, R. M. Sainz, R. Alonso-Arias, *Front. Immunol*. **2018**, *9*, 339. https://doi.org/10.3389/fimmu.2018.00339

[16] R. T. Selvi, A. P. S. Prasanna, et al. *Appl. Surf. Sci*. **2018**, *449*, 603–609.

[17] S. S. Nair, *Therapeut.* **2019**, *9*, 266–270. https://doi.org/10.22270/jddt.v9i1.2180

[18] I. O. Wulandari, V. T. Mardila, *Mater. Sci. Eng*. **2018**, *299*, 012064. https://doi.org/10.1088/1757-899X/299/1/012064

[19] A. Kumar, A. Vimal, et al. *Int. J. Biol. Macromol.* **2016**, *91*, 615–622. https://doi.org/10.1016/j.ijbiomac.2016.05.054

[20] F. S. El-banna, M. E. Mahfouz, et al. *Appl. Sci*. **2019**, *9*, 2193. https://doi.org/10.3390/app9112193

[21] Z. Chen, L. Xu, et al. *Food Res. Int.* **2020**, *137*, 109674. https://doi.org/10.1016/j.foodres.2020.109674

[22] C. Saikia, P. Gogoi, *J. Mol. Genet. Med*. **2015**, S4-006. https://doi.org/10.4172/1747-0862.S4-006

[23] H. Jafari, M. Hassanpour, et al. *Mater. Lett*. **2021**, *282*, 128818. https://doi.org/10.1016/j.matlet.2020.128818

[24] M. G. Amer, R. A. Karam, *Anat. Rec.* **2018**, *301*, 1454–1466. https://doi.org/10.1002/ar.23807

[25] A. A. Ozturk, H. T. Kiyan, *Microvasc. Res.* **2020**, *128*, 103961.

[26] A. K. Tuba, I. Gulcin, *Chem. Biol. Interact* **2008**, *174*, 27–37.

[27] D. R. Perinelli, L. Fagioli, *Eur. J. Pharm. Sci*. **2018**, *117*, 8–20. https://doi.org/10.1016/j.ejps.2018.01.046

[28] N. Annabi, E. Ebrahim Mostafavi, et al. *Artif. Cells Nanomed. Biotechnol.* **2018**, *46*, 938–945. https://doi.org/10.1080/21691401.2018.1439839

[29] L. Khorsandi, E. Mansouri, *Balkan Med. J.* **2016**, *33*, 252–257. https://doi.org/10.5152/balkanmedj.2016.150017

[30] G. Banuppriya, R. Sribalan, V. Padmini, et al. *Bioorg. Med. Chem. Lett.* **2016**, *26*, 1655–1659. https://doi.org/10.1016/j.bmcl.2016.02.066

[31] W. Muhammad, U. Naimat, et al. *RSC Adv.* **2019**, *9*, 29541–29548. https://doi.org/10.1039/C9RA04424H

[32] N. K. Jain, M. Nahar, *Methods Mol. Biol*. **2010**, *624*, 221–234. https://doi.org/10.1007/978-1-60761-609-2_15

[33] D. Segets, J. Gradl, R. K. Taylor, V. Vassilev, W. Peukert, *ACS Nano* **2009**, *3,* 1703–1710. https://doi.org/10.1021/nn900223b

[34] J. Van Embden, S. Gross, K. R: Kittilstved, E. D. Enrico Della Gaspera, *Chem.Rev.* **2023**, *123*, 271–326. https://doi.org/10.1021/acs.chemrev.2c00456

[35] X. He, H. Shou, X. Liu, K. Jia, *Polym. Bull*. **2022**, *79*, 4593–4605. https://doi.org/10.1007/s00289-021-03725-7

[36] J. W. Oh, S. C. Chun, M. Chandrasekaran, *Agron*. **2019**, *9*, 21. https://doi.org/10.3390/agronomy9010021

[37] S. Muthukumaran, R. Gopalakrishnan, *Opt. Mat*. **2012**, *34*, 1946–1953. https://doi.org/10.1016/j.optmat.2012.06.004

[38] H. Noei, H. Qiu, Y. Wang, E. Loffler, C. Woll, M. Martin Muhler, *Phys. Chem. Chem. Phys*. **2008**, *10*, 7092–7097. https://doi.org/10.1039/b811029h

[39] N. Masood, R. Ahmed, M. Tariq, Z. Ahmed, M. S. Masoud, I. Ali, R. Asghar, A. Andleeb, A. Anwarul Hasan, *Int. J. Pharm.* **2019**, *559*, 23–36. https://doi.org/10.1016/j.ijpharm.2019.01.019

[40] X. G. Zhang, D. Y. Teng, Z. M. Wu, et al. *J Mater Sci: Mater Med* **2008**, *19*, 3525–3533. https://doi.org/10.1007/s10856-008-3500-8

[41] P. Das, K. Ghosal, N. K. Jana, A. Mukherjee, P. Basak, *Mater. Chem. Phys*. **2019**, *228*, 310–317. https://doi.org/10.1016/j.matchemphys.2019.02.064